DYNA
http://dyna.medellin.unal.edu.co/

UNIVERSIDAD NACIONAL DE COLOMBIA

Relationship between climate variability and mass removal processes. Tunja-Páez case study

July Katerine Rojas-Mesa, Luis Carlos Leguizamón-Barreto & Luis Alfredo Vega-Báez

Facultad de Ingeniería, Universidad Pedagógica y Tecnológica de Colombia, Tunja, Colombia., july.rojas@uptc.edu.co, luiscarlos.leguizamon@uptc.edu.co, luis.vega@uptc.edu.co

Received: June 7th, 2024. Received in revised form: September 13th, 2024. Accepted: September 30th, 2024.

Abstract
This article focused on the relationship between the influence of climatic variables and seismic activity in the dynamics of slopes that presented mass removal phenomena in the case study: Tunja-Páez Corridor. This analysis was carried out through the application of a probabilistic model that integrated parameters of soil resistance, seismic activity, and accumulated precipitation to establish the definition of rainfall thresholds obtained from the rainfall records preceding each of the removal events. This model used first order, second moment FOSM, and the Poisson distribution of probabilistic foundations to estimate the probability of failure of given slope. Additionally, the change in precipitation in the years 2040, 2070, and 2100 as defined by forecasts of Climate Change (CC) according to IDEAM were used to compare the effects on the probability of soil saturation.

Keywords: climate variability; mass removal; precipitation; seismic activity; road infrastructure.

Relación entre la variabilidad climática con procesos de remoción en masa. Caso de estudio Tunja-Páez

Resumen
El presente artículo tuvo como enfoque relacionar la influencia de variables climáticas y la actividad sísmica en la dinámica de los taludes que presentaron fenómenos de remoción en masa en el caso de estudio: vía Tunja-Páez. Este análisis se realizó mediante la aplicación de un modelo probabilístico que integró parámetros de resistencia del suelo, actividad sísmica y la precipitación acumulada para establecer la definición de umbrales de lluvia obtenidos de los registros de lluvia antecedente a cada uno de los eventos de remoción. Dicho modelo utilizó fundamentos probabilísticos de primer orden y segundo momento FOSM y la distribución de Poisson, con el fin de estimar la probabilidad de falla del talud, además se involucró el cambio de las precipitaciones en el año 2040, 2070 y 2100 definidas por pronósticos del Cambio Climático (CC) según el IDEAM con el propósito de comparar las afectaciones en la probabilidad de saturación del suelo.

Palabras clave: variabilidad climática; remoción en masa; precipitación; actividad sísmica; infraestructura vial.

1 Introduction

The variations presented in the climatic context worldwide have unleashed a series of territorial effects that may impact society in various ways. These impacts include fires, an increase in sea level, extreme weather events, and increases in temperature and precipitation, among others [1]. The change in temperature is shown by the increase of 1°C on a global scale from 1880 to 2017 which is equivalent to a gradual increase of 0.2°C per decade. This scenario is discouraging when the Intergovernmental Panel on Climate Change [2] warns of a global warming of 1.5°C by the year 2040.

Additionally, an average increase of 19 cm in the mean sea level between 1901-2010 was recorded and according to the World Meteorological Organization (WMO) it is expected that this level will reach 58 cm by the year 2100 [3]. These kinds of effects are attributed to greenhouse gas (GHG) emissions discharged into the atmosphere since the industrial revolution as stated by the IPCC. Even though

How to cite: Rojas-Mesa, J.K., Leguizamón-Barreto, L.C., and Vega-Báez, L.A., Relationship between climate variability and mass removal processes. Tunja-Páez case study. DYNA, 91(234), pp. 34-43, October - December, 2024.

Colombia does not contribute significant amounts of emissions into the atmosphere in this type of discharges, it is affected by the climatic variations that this phenomenon implies.

An example of this occurred in 2010 when a rainy event known as the La Niña Phenomenon left 21,300 people affected, 771 homes destroyed, 50 dead, and 52 injured due to mass movements triggered by heavy rainfall throughout Colombia [4]. By taking into consideration the predictions made by the Institute of Hydrology, Meteorology, and Environmental Studies (IDEAM), it is estimated that by 2040 there will be a reduction in precipitation of 30% in the Caribbean region and Amazon, while for the central zone, which includes Cauca, the Coffee Region, Huila, Tolima, and Boyacá, they will increase by more than 30% [5].

The effect of hydroclimatic factors in the activation of historical disasters in Colombia had an incidence of 88% between 1998 and 2016. According with the National Planning Department (DNP), 15% of the incidences corresponded to mass movements throughout the country [6]. Regarding the regional scenario, Boyacá ranks fourth within Colombia as the department with the greatest population exposed to hydroclimatic threats with 59.6% [7]. For the period between 2014 and 2018, 75 mass movements associated with landslides were registered according to a report from the Cámara de Comercio Tunja, Duitama, and Sogamoso [8].

The problems generated by the activation of processes in mass removal brings with it social and economic effects [9], which slow down the development of the territory in terms of transport and connectivity [10]. Colombia has been working on the formulation of strategic risk management plans to mitigate the impact of such events [11]; however, there is no evidence of an analysis in the Department of Boyacá. This is especially true of determining the effects of climatic variables in terms of precipitation and seismic activity on the activation of mass removal phenomena on the slopes that make up the Tunja-Páez road corridor.

The current study incorporates a catalog of mass removal processes obtained from the Mass Movements Information System "SIMMA" from the Colombian Geological Service generated in the study area. This catalog is related to the accumulated daily precipitation and the climate change scenarios of 2040, 2070, and 2100 which allow an estimation of the probability of slope failure. The seismic activity of the area is included through the application of deterministic methods and probabilistic techniques which are represented in Geographic Information Systems [12,13] such as Quantum GIS. The results obtained in this study can be considered an initial phase for estimating the threat in linear projects in the region and provide criteria on the formulation of mitigation and/or adaptation measures for drainage and containment projects related to road infrastructure in the framework of climate change forecasts.

2 Materials and methodology

2.1 Description of the study area

The Tunja-Páez road corridor is 118 km long and is located in the department of Boyacá on the Eastern Cordillera in the An-dean Region and crosses the following municipalities in order from north to south: Tunja, Ramiriquí, Zetaquira, Miraflores, and Páez (Fig. 1). It is identified as Route 60 of the National Road Network and also has a rugged mountainous relief with elevations that vary between 1,300 and 3,000 meters above sea level. These reliefs make it difficult for the geometric layout in some sections and results in areas of instability on the slopes. The Tunja-Páez road corridor has an area of influence of 1,700 km2 and an estimated 53,000 inhabitants. It is currently paved between Tunja and Miraflores according to the National Institute of Roads [14].

2.2 Information collected from mass movements

The information on the mass movements of the department of Boyacá is obtained from the Catalog and Inventory of the Mass Movements Information System (SIMMA) of the Colombian Geological Service (SGC) and the inventory of mass movements of the Georeferencing platform (HERMES) from the National Institute of Roads (INVÍAS). 2174 data points of mass removal events are collected for the department of Boyacá between 1972 and 2020. With the layer of the study road (Tunja-Páez) in QGis, a grid is created that frames the entire corridor road through a rectangular strip 12 km wide and 60 km long, made up of cells of 1 square km. Only mass movements that were limited by the grid are considered which corresponded to 271 events that affect the Tunja-Páez road corridor (Fig.1).

2.3 Information collected about precipitation

A database of the daily precipitation was obtained from the pluviometric stations of IDEAM close to the recorded mass movements as shown in Table 1.

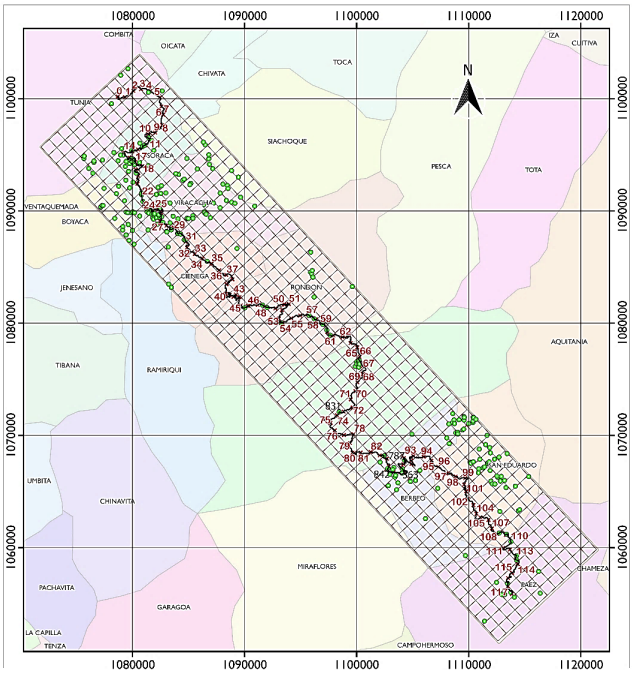

Figure 1. Mass movements recorded in the study area via Tunja-Páez
Source: Authors

Table 1.
Hydroclimatological stations used for the analysis of the precipitation variable

Station	Code	Category*	Latitude (N)	Longitude (O)	Period
Páez	35080050	P	5.096361	-73.053222	1975-2020
Zetaquira	35080010	P	5.282972	-73.169277	1957-2020
Rondón	35085020	CO	5.358416	-73.203611	1970-2020
Ramiriquí	35070010	P	5.399527	-73.332972	1957-2020
Villa Luisa	35075030	CO	5.422222	-73.349416	1981-2020
Teatinos	35070310	P	5.422822	-73.375777	1990-2020
Pila la finca	24030420	P	5.518916	-73.310722	1992-2020
Campo Hermoso	35085050	CO	5.034500	-73.103666	1986-2020
El Vivero	35085040	CO	5.192555	-73.144777	1984-2020
Camp Buenavista	35080030	P	5.183722	-73.086722	1962-2020
UPTC	24035130	CO	5.553611	-73.355277	1962-2020

Category: *P: fluviometric, *CO: Ordinary Climate
Source: The authors

2.4 Geological information collected

The road from the city of Tunja to the Municipality of Zetaquira is located on the Soapaga regional fault and the predominant materials in the area up to the municipality of Páez correspond to colluvial deposits [15]. These masses are composed of clay matrix blocks of colluvial origin. The slopes present undermining events at the base due to the natural channels produced by the high intensity of rainfall in the area. The current study considers the use of the geological units present in the department of Boyacá that frame the study corridor in order to identify the geotechnical parameters that can condition the stability of the soils.

Table 2.
Resistance parameters identified in the Tunja-Páez roadway corridor

Symbol UG	Description	Soil unit weight (KN/m^3)		Internal friction angle (°)		Cohesion (KPa)	
		μ	Σ	μ	σ	μ	σ
Kpgt	Claystones and siltstones with coal seams	19.02	0.95	29.20	2.92	10	5
Ksm	Quartz sandstones, siliceous mudstones, shales and shales. limestone banks.	20.71	1.04	30.18	3.02	10	5
Ngc	Sandstones with intercalations of claystones, conglomerates and locally pyroclastic	19.02	0.95	29.20	2.92	10	5
Pgc	Polymictic conglomerates, quartz sandstones and claystones.	19.02	0.95	29.20	2.92	10	5
Pgt	Claystones with intercalations of clayey to conglomerate sandstones and coal beds.	20.71	1.04	30.18	3.02	10	5
Kim	Limestone and calcareous mudstone, sandstone and claystone conglomerates.	18.63	0.93	28.10	2.81	49.03	24.52
Kit	Quartz sandstones with intercalations of mudstones and limestones.	18.00	0.90	26.00	2.60	35	17.50

Source: The authors

According to the geological map of Boyacá, each type of soil was assigned the resistance parameters corresponding to the unit weight of the soil (γsoil in kN/m3), cohesion (c in kPa), angle of internal friction of the soil (ϕ in degrees), and the average slope of the land (α in degrees) in the areas where landslides occur (Table 2). The values presented in each of the soil properties are obtained from road improvement projects carried out by the Tecnoconsulta Group in INVÍAS studies [14].

2.5 Applied methodology

The current study used the methodology suggested by [16] which considers the infinite slope model that allows forecasting the probability of the failure of a slope (PFT) involving the behavior of accumulated daily rainfall to each slope process mass removal. This method is based on the safety factor equation, whose expression involves the soil resistance parameters of the geological units of the study area, the height of the water table, the topography of the area to be analyzed in terms of inclination of the slopes, and the values of effective peak acceleration (PGA).

Within the bibliographic review of the methodologies that relate rain and seismic activity as triggers of mass removal processes in terms of probability of failure, this methodology turns out to be practical for roads exposed to this type of phenomena because it can be carried out a sensitivity test in the rainfall equations preceding each removal process involving climate change scenarios to try to establish probabilities of saturation and total failure throughout the Vail corridor under study.

The possible relationship of climatic variables with mass removal processes is determined by the probability of total annual failure of a slope (PFA) as applied by [17] by considering the precipitation and earthquake variables. This model estimates the probability that the safety factor (FS) is less than 1.0, indicating a slope failure condition.

The expression evaluates a scenario in dry and saturated conditions by estimating fault surfaces and water tables at different heights. It is limited by the fact that this expression doesn't take into account the effect of soil saturation where these types of movements occur due to the complexity that this implies. Historical rainfall averages in the area of study are included in order to estimate the rainfall threshold that can generate these removal events and therefore give an estimate of soil saturation. The estimation of the probability of slope failure expressed by eq. (1) depends on the mechanical characteristics of the soils and their relationship with the rainfall and seismic activity in the area.

$$P_{ft} = P_{fs} * P_s + P_{ns} * (1 - P_s) \quad (1)$$

Where: Pft = probability of total failure of the slope, Pfs = probability of failure of the slope due to an earthquake in saturated condition, Ps = probability that the soil is saturated, Pns = probability of failure due to earthquake in unsaturated condition, and (1-Ps) = probability that the soil is not saturated.

To determine the probability of total failure of the slope, an estimation of the marginal probability that the soil is saturated, and an emphasis on the estimation is used because the process is carried out empirically to determine the thresholds of rain that can activate mass movements. It is also very complicated to analyze the phenomenon of infiltration and moisture content present in the soils in question. Studies carried out in other areas of Colombia by [18-20] have defined critical rainfall thresholds by considering short-term rainfall and long-term rainfall for each of the mass movements detected.

2.6 Precipitation inference

The generation of rainfall thresholds that can be associated with the appearance of mass movements, are obtained through a mix of short-term rainfall (LA) and long-term rainfall (LAA), which allows dispersion scenarios to be created and compared to rainfall averages and the occurrence of mass removal processes [19].

The relationship between climate variability in terms of precipitation and mass shedding processes lies in the definition of rainfall thresholds for the study area corresponding to the Tunja-Páez roadway corridor. These thresholds were defined by combining short-term rainfall (LA) to the removal event for 1, 3, 5, and 7 days with long-term rainfall (LAA) at 5, 10, 15, 30, 60, and 90 days [21]. These combinations generate 24 scenarios that represent the behavior of rainfall in the area and can be associated with the generation of mass movements. The proposed rainfall threshold for the occurrence of mass movements is represented in Fig. 2.

Fig. 2 contains three representative regions of antecedent rainfall (A, B, and C) for the mass removal events recorded in the study area [18]. Region (A) frames the removal processes possibly activated by little rain; however, these events cannot be related to short-term rainfall, but rather to geological factors in the area.

Region (B) is defined by events triggered by 15 days of accumulated rainfall less than 160mm followed by accumulated rainfall 3 days prior to the activation of the removal process. This condition could signal a dangerous scenario for unstable slopes. Finally, region (C) represents the area where the heaviest precipitation occurs with an accumulation of more than 15 days. The events that occur in this region can be triggered by soil saturation due to a water storage for several days. These regions are described in Table 3.

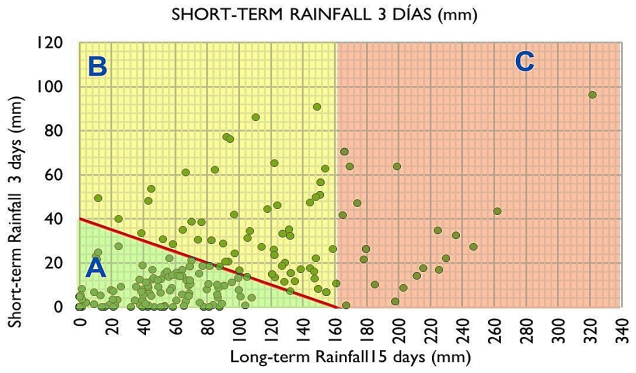

Figure 2. Rain threshold for the Tunja-Páez road
Source: The authors

Table 3.
Description of the representative regions of Fig.2

Region	Description
A	$P_{15} < 40$mm does not exceed threshold
B	$0 < P_{15} < 160$mm exceed threshold
C	$P_{15} > 160$mm exceed threshold

Source: The authors

The behavior of the rains in all the scenarios analyzed allows for the establishment of the definition of thresholds for LA of 3 days and LAA of 15 days, since this combination presents the least dispersion of records of mass removal presented and in turn concentrates the majority of the events (82%) of mass movements between the thresholds of LA of 40 mm and LAA of 160 mm. This indicates that 18% of the events occurred under rainy conditions greater than 40 mm and that the rain on the days prior to the appearance of each of the mass movements can be decisive in the occurrence of surface mass events that are already directly related to the regime of short rainfall. The proposed rainfall threshold Fig. 2 that can cause mass movements in the Tunja-Páez road is expressed by eq. (2).

$$P_3 = -0.25P_{15} + 40mm; \quad con \quad 0 < P_{15} < 160mm \qquad (2)$$

Where: P3: Accumulated rainfall 3 days prior (mm), P15: Accumulated rainfall 15 days prior to the 3 days in (mm).

According to the equation of the straight line, when P15>160mm (defined by the red border line), a very small, accumulated precipitation of 3 days (P3) can trigger a mass removal process. According to [22], it represents a propitious condition for the infiltration of water into the soil layers and generates a critical condition in the event that said accumulated rain increases the pore pressure and therefore reduces the bearing capacity of the soil, thus activating the mass movements. The soil is predicted to be saturated when the 3-day accumulated rainfall exceeds the threshold rainfall calculated by P3 and determined by eq. (3).

$$Ll_{3m} \geq Ll_3 \qquad (3)$$

Where, Ll3m: accumulated rainfall of 3 days LA (mm), Ll3: P3 threshold (mm). In order to fulfill the condition established in eq. (3), a new series is generated that relates the accumulated rainfall of 3 days (LA3) and the preceding accumulated rainfall of 15 days (P15) by means of the mobile rain windows technique. Here, LA3 corresponds to the sum of the precipitation of 3 consecutive days which starts from the first precipitation record including the day on which the event occurs to obtain the first record, the process is repeated adding the following 3 rain records shifting the calculation from day to day to the last record of that series. Finally, Ll3m is the result of the partial summations of the moving rain windows which is repeated for P15.

When the condition of eq. (3) is met, a count is made of the times that the threshold was exceeded in the generated series, which is called occurrences. These occurrences, when divided by the total rainfall records, represents the probability of soil saturation [22]. According to the studies carried out by [17], the probability of soil saturation is related to the probability of annual failure (due to the action of the rains) in

terms of a conditional probability that a landslide occurs at the site (Ls) given that the daily precipitation exceeds the slope failure threshold (RT) as defined by eq. (4).

$$P(L_S|R > R_T) = \frac{ND_S}{ND_T} \quad (4)$$

Where: P(LS | R>RT) = conditional probability that a landslide occurs on the road given that daily precipitation (R) exceeds the critical rainfall threshold, NDS = number of times the threshold is exceeded at the site of the slope, NDT = total number of times the threshold is exceeded in the entire road corridor. This allows us to calculate the temporary probability of failure (PT) expressed by eq. (5) using the Poisson distribution which considers the number of events that exceed said threshold in a time t which refers to the years of record, corresponding to 47 years for the current study.

$$PT = P(X \leq x) * P(L_S|R > R_T) \quad (5)$$

Taking into account that PT= temporal probability of failure of each of the critical slopes and P (X≤x) = Poisson distribution defined as the annual probability of n failures occurring with λ for 47 years of records.

By considering the location of the mass removal points in the road corridor and its area of influence, the conditional probability and the temporary probability of failure of each of the critical points and the probability of saturation of the soil (Ps) can be established. Through the sum of the partial (temporary) probabilities along the Tunja – Páez road, this probability is equivalent to 91.90%.

The determination of the probability of soil saturation exposed in Table 4 is represented in Fig. 3 according to the performance of an interpolation in the Quantum Gis (QGis) software. This allows the probabilistic values in each row of the 1km grid within the area of influence of the Tunja-Páez road.

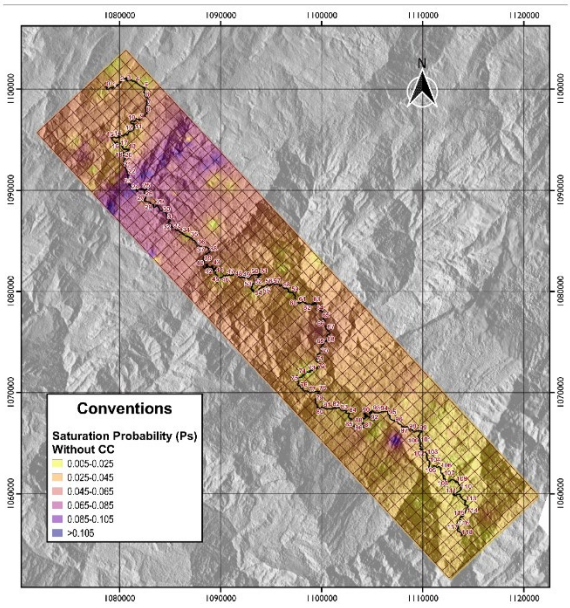

Figure 3. Probability of Saturation without precipitation scenario due to Climate Change (CC)
Source: The authors

Table 4.
Temporary probability of saturation of the Tunja-Páez road by row of the 60 km grid

Number	No. Events	Nf/R>RT	P(Ls/R>RT)	λ	P(X≤x)	PT
1	2	1	0.00629	0.0213	1.00	0.00629
4	4	2	0.01259	0.0426	1.00	0.01259
5	9	8	0.05036	0.1702	1.00	0.05036
6	7	4	0.02518	0.0851	1.00	0.02518
7	2	2	0.01259	0.0426	1.00	0.01259
8	12	3	0.01888	0.0638	1.00	0.01888
9	2	2	0.01259	0.0426	1.00	0.01259
10	15	11	0.06924	0.2340	1.00	0.06924
11	21	16	0.10071	0.3404	1.00	0.10071
12	21	9	0.05665	0.1915	1.00	0.05665
13	4	3	0.01888	0.0638	1.00	0.01888
14	14	10	0.06295	0.2128	1.00	0.06295
15	12	9	0.05665	0.1915	1.00	0.05665
16	3	2	0.01259	0.0426	1.00	0.01259
17	2	2	0.01259	0.0426	1.00	0.01259
18	2	1	0.00629	0.0213	1.00	0.00629
24	5	5	0.03147	0.1064	1.00	0.03147
25	5	4	0.02518	0.0851	1.00	0.02518
26	1	1	0.00629	0.0213	1.00	0.00629
27	2	1	0.00629	0.0213	1.00	0.00629
29	2	1	0.00629	0.0213	1.00	0.00629
30	3	3	0.01888	0.0638	1.00	0.01888
34	7	6	0.03777	0.1277	1.00	0.03777
42	2	2	0.01259	0.0426	1.00	0.01259
43	11	5	0.03147	0.1064	1.00	0.03147
44	16	5	0.03147	0.1064	1.00	0.03147
45	11	1	0.00629	0.0213	1.00	0.00629
46	1	1	0.00629	0.0213	1.00	0.00629
47	7	4	0.02518	0.0851	1.00	0.02518
48	11	2	0.01259	0.0426	1.00	0.01259
49	3	1	0.00629	0.0213	1.00	0.00629
50	8	3	0.01888	0.0638	1.00	0.01888
51	2	2	0.01259	0.0426	1.00	0.01259
53	3	1	0.00629	0.0213	1.00	0.00629
54	1	1	0.00629	0.0213	1.00	0.00629
55	2	2	0.01259	0.0426	1.00	0.01259
56	2	1	0.00629	0.0213	1.00	0.00629
57	2	2	0.01259	0.0426	1.00	0.01259
58	5	5	0.03147	0.1064	1.00	0.03147
59	1	1	0.00629	0.0213	1.00	0.00629
60	1	1	0.00629	0.0213	1.00	0.00629
		TOTAL				**0.919**

Source: The authors

2.7 Climate change scenarios regarding the variability of precipitation

Climate change scenarios in terms of precipitation provide information on the increase or decrease in precipitation in any region of the country. This information was obtained from the IDEAM open data portal in order to observe the areas where these changes are evident in the department of Boyacá. These climate change scenarios correspond to periods of 30 years grouped as follows: from 2011 to 2040; 2041 to 2070, and 2071 to 2100 and were built from the behavior of rainfall in the period between 1976 and 2005. These scenarios present variations ranging from -9% to over 40% depending on the distribution of daily rainfall throughout the department. Considering the above, a new rain series is generated (one series per scenario) using the daily precipitation data modified by the variations that may occur. This allows the thresholds that can trigger movements to be obtained for each climate change scenario and applied to the moving windows process. For the purposes of this study, we intend to analyze the changes presented in the recorded rainfall which affecting them by the critical percentage variation. The results obtained for each scenario are listed in Table 5.

Table 5.
Failure thresholds for each Climate Change scenario

Characteristics	2040	2070	2100
Failure Threshold Equation	P_3= -0.14P_{30}+40mm	P_3= -0.18P_{30}+45mm	P_5= -0.17P_{30}+45mm
No. Data between thresholds	141	147	156
% Data between thresholds	59	54	58
% Probability of roadway saturation Ps	95.40	91.86	97.23

Source: The authors

Table 6.
Temporary probability of saturation of the Tunja-Páez road for each of the climate change precipitation scenarios

Scenario	Ps for the entire roadway (%)	Change (%)
without CC	91.90	
2040	95.40	+3.5
2070	91.86	- 0.04
2100	97.23	+5.3

Source: The authors

To analyze the behavior of precipitation at different time scales and its influence on the Tunja-Páez road, a new series of accumulated daily precipitation has been gathered including this variation for each of the new Climate Change scenarios for the years 2040, 2070, and 2100. This information allows us to compare the probability of saturation in the three scenarios with respect to the current scenario as represented in Table 6.

Each future precipitation scenario presents a marginal change as shown in Table 6. Here, the difference in probabilities for each one with respect to the scenario without Climate Change varies between 0.04% and 5.33%, the latter being the one with the greatest increase in the probability of saturation and corresponding to the year 2100.

2.8 Influence of seismic activity

Seismic activity is associated with the possible occurrence of removal processes on the slopes of unstable areas through the application of the limit equilibrium method [23] in which the safety factor for the infinite slope is considered in each one of the areas of the grid that frames the road corridor. This process allows the probability of slope failure due to seismic action (Pfs) to be calculated by incorporating the parameters of soil resistance, rainfall, and seismic activity [17]. The data on the resistance parameters of the study soils were collected through the layers of the Geographic Information Systems of the Colombian Geological Service, Corpoboyacá, INVÍAS, and other complementary studies. The information to be used corresponds to lithological and geological units obtained from the Geological Map of Boyacá, the Digital Elevation Model DEM, and the seismic hazard layer of Boyacá to obtain the design PGA with respect to the place of each mass movement.

According to the infinite slope methodology, the probabilities of failure of slopes that can present mass movements are calculated according to the return period of the PGA obtained and reported in the General Seismic Hazard Study of Colombia [24]. For the current case study, this corresponds to 475 years with an acceleration value of 0.2g, that is, the multiplying factor will be 1/475 to find the probability of failure of the annual slope given a probability of total failure of the system. Assuming that the resistance parameters and the SF behave according to a standardized normal distribution with a mean of 0 and a standard deviation of 1, eq. (6) is obtained, which relates the aforementioned variables.

$$FS = \frac{c}{\gamma H cos\alpha(sin\alpha + PGA cos\alpha)} + \frac{(\gamma H - \gamma_W Hw) cos\alpha \tan\phi}{\gamma H(sin\alpha + PGA cos\alpha)} \quad (6)$$

Where c= soil cohesion [kPa or kN/m^2], γs= unit weight of soil [KN/m^3], γw= unit weight of water [KN/m^3], H= height of the failing zone [m], Hw= height of the water from the fault surface [m], ϕ = Angle of internal friction of the ground [°], α= average slope of the terrain [°], and PGA= acceleration produced by the earthquake defined by 0.2g. The variables that make up eq. (6), are assumed for H and Hw in the current study in order to analyze the sensitivity of the slope failure probability when failure surface heights (H) of 5m, 10m, and 20m are considered along with water table depths (Hw) of 0m, 3m, and 5m. For the purposes of this analysis, the 5m failure surface is considered since it is related to surface mass movements [25]. As for the heights of water from the failure surface, they are set at 0m and 5m to estimate the probability of failure of the slope during wet conditions and in saturated condition, respectively.

2.9 Slope failure probability

The probability of failure of a slope at a critical point depends on the exceedance of the intrinsic variables of the model. For rainfall, this was calculated through the exceedance of the critical rainfall threshold. However, for the purposes of analyzing the relationship between seismic activity and the generation of mass removal processes, it is determined as the probability that FS is less than 1. This probability is evaluated by means of a reliability index (β) expressed in eq. (7), which considers the effect of the uncertainty of the model representing the number of standard deviations between the most probable value of the factor of safety E(FS) and the factor of safety equal to 1 [FS=1], [17].

$$\beta = \frac{E[FS] - 1}{\sigma[FS]} \quad (7)$$

Where E[FS] = expected value of the factor of safety and σ[FS]= standard deviation of the factor of safety. The estimation of the probability of failure in unsaturated and saturated conditions is determined by the area under the curve of the probability density function of the SF with values less than 1 when applying the normal distribution and the Bae-statistical technique of [26].

The use of the Taylor series to calculate the probability distribution of a function with "n" number of random variables requires the values of the moments of the statistical

distributions of the variables that make up the function, in this case of 1st order and 2nd moment (FOSM), equivalent to the expected value E[FS] and the variance V[FS] of the safety factor. The FOSM method determines the partial derivatives of the variables $\bar{X}i$ =c, ϕ and γ_{soil}, in order to calculate the variance and subsequently the standard deviation [27], as observed in Eq. (8)-(9).

$$E[F] = F(\bar{X}_1, \bar{X}_2, \ldots \bar{X}_N) \quad donde \ \bar{X}_i = E[Xi] \tag{8}$$

$$V[F] = \sum_{i=1}^{N} \left(\frac{\partial F}{\partial X_i}\right)^2 * V(X_i) \tag{9}$$

The function F is evaluated for the mean values of all the variables considered in the calculation of FS. Once the probabilities that make up eq. (1) have been determined, the probability of total slope failure (PFT) can be calculated.

2.10 Results and discussion

The model used for the total probability of slope failure is calculated by determining the E[FS]. This is done by taking the respective average values of the mechanical characteristics of the soils in the area where the Tunja-Páez corridor extends for each of the failure surfaces (H= 5m, 10m, and 20m). Each failure surface (H), in turn contains a calculation of the safety factor for each estimated water table by taking into consideration the different heights of the water level (Hw= 0m, 3m, and 5m). When the failure surface is 5m, the SF decreases in the first 40 kilometers of the road corridor. When the water table rises to 5m with SF values less than 0.5 on the other hand, the last 40 kilometers show values of FS>1.0. The comparison allows for the understanding the variation of the safety factor when it is affected by the water table and the failure surface in the entire road corridor. The changes are presented in Tables 7 and Table 8 taking as reference the failure surface at 5m and the height of the water level of Hw= 0, 3, and 5m respectively.

A decrease in FS is observed on average of 20% when the failure surface is 10m and 30% when this depth is 20m when taking the failure surface at 5m as a reference. For the case of the 5m failure surface, a decrease in the safety factor of 16% is observed when the assumed water table rises to 3m and 26% when the height of the water reaches 5m. This behavior is due to the findings by [28] and other authors when they relate the decrease in the safety factor with the increase in pore pressure and the loss of soil stability caused by the possible saturation of the soil. According to the above, the critical conditions of the soil are evaluated when the water level is 5m corresponding to a saturated condition and in a humid condition when this level is 0m. This allows us to define the probability of slope failure when the soil is saturated and when it is not by applying the normal distribution. This normal probability is calculated taking into account the partial derivatives of the soil resistance parameters through the FOSM method. This determines the variance and standard deviation of the safety factor (eq. 7, 8) in order to evaluate the comparison of this variable with a FS=1.

This process allows us to obtain the probabilities per earthquake for an unsaturated condition (Pfns) in Fig. 4 from which values between 44% and 80% are obtained and for a saturated condition (Pfs) in Fig. 5 with probabilities between 47% and 94%. In critical terms, the probability of failure between 47% and 94% evaluated in a saturated condition (Hw=5m) is related to terrain slopes that range between 38° and 42°. This situation occurs in areas where they present higher probabilities of soil saturation with values close to 30%. Considering that the probability of soil saturation is determined by eq. (4)-(5), a minimum annual saturation probability of 0.63% and a maximum of 10.13% are observed. This corresponds to partial probabilities within the road corridor; however, when evaluated in terms of probability of saturation (Ps) for the entire Tunja – Páez road, it has a value of 91.90% which is considered in the calculation of the Total Failure Probability (PFT) of the slopes in the study area.

Table 7.
Safety factor changes for (H=10m and Hw=0, 3, and 5m)

E [FS] Failure Surface H=10m		
Hw=0m	Hw=3m	Hw= 5m
-0.230	-0.154	-0.104
-24%	-19%	-15%

Source: The authors

Table 8.
Safety factor changes for (H=20m and Hw=0, 3, and 5m)

E [FS] Failure Surface H=20m		
Hw=0m	**Hw=3m**	**Hw= 5m**
-0.344	-0.232	-0.156
-36%	-29%	-22%

Source: The authors

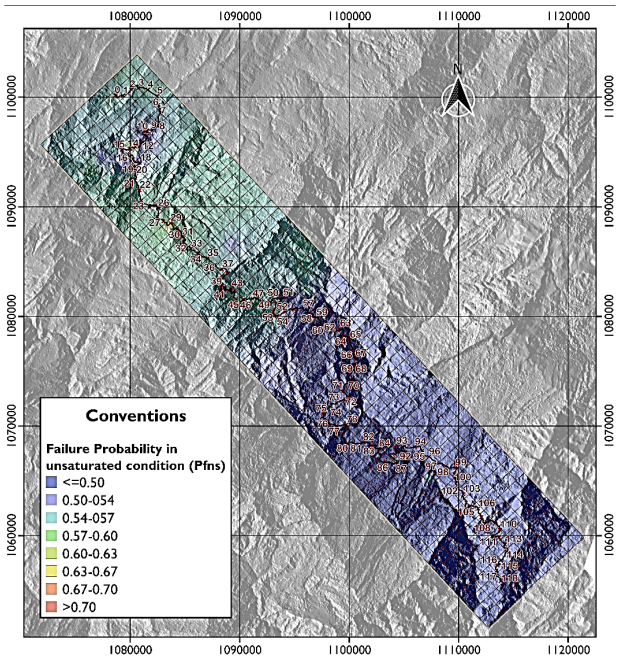

Figure 4. Failure probability due to earthquake in unsaturated condition (Pfns)
Source: The authors

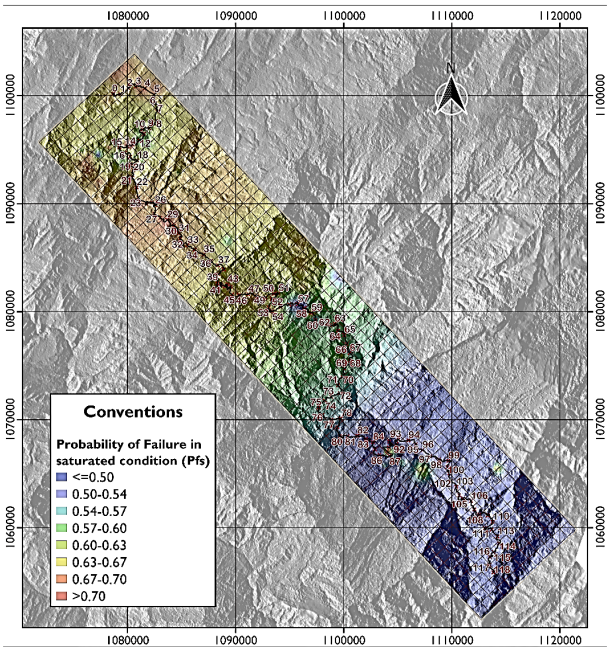

Figure 5. Failure probability due to earthquake in saturated condition (Pfs)
Source: The authors

With the application of eq. (1), the probability of total failure of the PFT slopes present in the Tunja-Páez road is estimated, where values between 46.42% and 93.02% are obtained. When these values are impacted by the annual probability of an earthquake whose value corresponds to 0.2% for a return period of 475 years (design PGA). According to the study from Colombia [24], the annual failure probabilities (PFA) range from 0.0977% to 0.1958% which make up an annual probability of failure in the entire corridor of 32.83%. These annual failure probabilities in terms of landslide hazards can be considered low based on the criteria of [29] and their classification of PFanual for values between 0.2% and 0.02%. According to a diagnosis carried out in the field along the entire Tunja-Páez corridor, 10 critical points are identified that present slopes between 40° and 50° according to the map of slopes from the Lidar images obtained directly in the field using drone flights. These instability zones are presented in Table 9 and the annual failure probability (PFA) is observed for each of the points.

The probabilities of total slope failure (PFT) and total annual slope failure (PFA) presented in Table 9 represent the partial probability of the area where each mass movement was recorded, but not that of the entire road corridor. The probabilities and critical points identified are represented in Fig. 6. According to an interpolation carried out with the PFT results in the QGis program, the behavior of the probability is graphically represented in the entire area of the Tunja-Páez road corridor.

Fig. 6 represents the PFT in the Tunja-Páez road corridor without being affected by the Saturation Probabilities (Ps) of the CC. The highest PFT occurs in the first 55 kilometers of the road belonging to the municipalities of Soracá (PR 4+000), Boyacá – Boyacá (PR 14+000), Ramiriquí (PR 23+000), and Quebrada Honda (PR 54+000) with values above 63%. Meanwhile, PFTs below 47% occur between the municipalities of Miraflores (PR 86+000) and Páez (PR 118+000).

The picture changes when the PFT is recalculated using eq. (1) with the Ps for the three CC scenarios (2040, 2070, and 2100) (Table 5) whose results are presented below (Tables 10 and Table 11).

Table 9.
Critical points obtained in the Tunja-Páez corridor

No.	Marker	Length (m)	Location	PFT (%)	PFA(%)	Contention and/or drainage work
1	PR 13+625	100	Soracá	93.02	0.1958	Failing retaining wall and failing drainage
2	PR 29+583	200	Ciénega	93.02	0.1958	Stone retaining wall and blocked drainage pipes
3	PR 45+581	80	Rondón	64.61	0.1361	No infrastructure
4	PR 57+745	60	Rondón	64.61	0.1361	Box culvert
5	PR 58+925	50	Rondón	54.74	0.1152	Failing retaining wall
6	PR 60+880	220	Zetaquira	48.85	0.1028	Drain in concrete/no retaining wall
7	PR 83+393	50	Zetaquira	46.73	0.0984	Failing retaining wall
8	PR 89+686	40	Miraflores	46.42	0.0977	Box culvert and failing retaining wall
9	PR 108+990	100	Páez	46.83	0.0986	No drainage/retaining wall
10	PR 113+330	200	Páez	46.83	0.0986	No infrastructure

Source: The authors

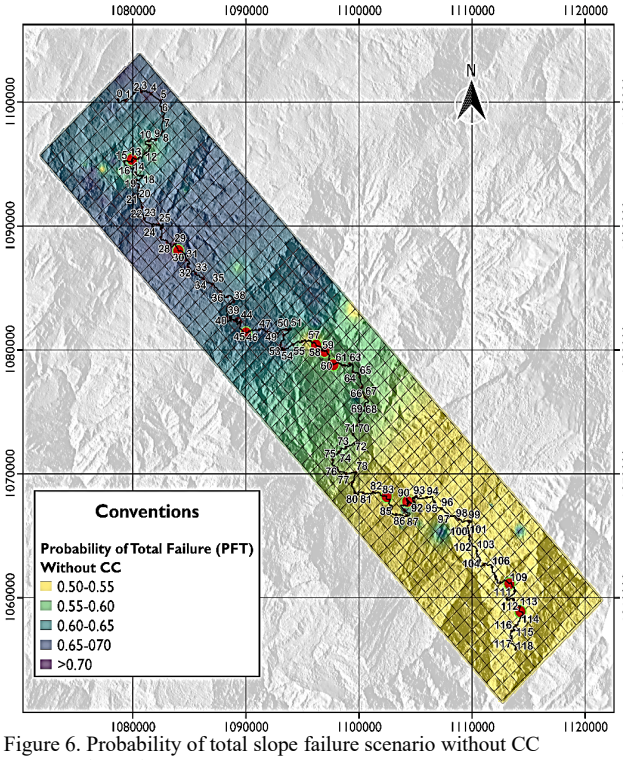

Figure 6. Probability of total slope failure scenario without CC
Source: The authors

Table 10.
Total Failure Probability (PFT) of the Tunja-Páez road for each of the Climate Change (CC) scenarios

Scenario CC	PFT Min. (%)	PFT Max. (%)	PFTA Min. (%)	PFTA Max. (%)
Without	46.42	93.02	0.0977	0.1958
2040	46.50	93.52	0.0979	0.1969
2070	46.42	93.02	0.0977	0.1958
2100	46.54	93.77	0.0980	0.1974

Source: The authors

Table **1**.
Total Failure Probability (PFTA) for the entire Tunja-Páez road in each of the Climate Change (CC) scenarios

Scenario CC	∑ PFTA (%)	Difference (%)
Without	32.83	0.00
2040	32.98	+0.15
2070	32.83	0.00
2100	33.06	+0.23

Source: The authors

Table 10 relates the PFT of each event that occurred in the Tunja-Páez road corridor and in turn the probabilities of total annual failure (PFTA) by involving the annual probability per earthquake. However, Table 11 shows the difference of the PFTA between scenarios referencing the scenario without Climate Change and for the entire road corridor (sum of partial PFTAs of each event).

In Fig. 6, 7, the probability of total failure (PFT) is represented in the area of the study road corridor through the interpolation of the results obtained for the scenario without the effects of Climate Change and the year 2040. The effect of rainfall on the PFT between the scenario without Climate Change and the three CC scenarios (2040, 2070, and 2100) is relatively low. Fig. 7 can represent the behavior of the three CC scenarios since the PFT has a similar behavior.

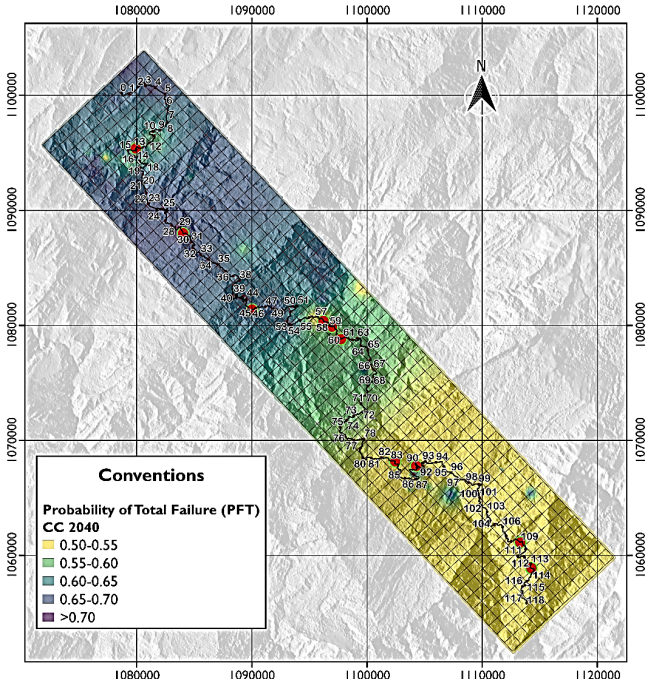

Figure 7. Probability of total slope failure scenario year 2040
Source: The authors

2.11 Conclusions

The probabilistic model based on the limit equilibrium method allows us to determine the existing relationship in a practical way between the climatic variables with mass removal processes and taking into consideration the seismic activity in the deterministic calculation of the safety factor obtained from the mechanical parameters of the soils present in the Tunja-Páez road corridor.

It is important to clarify that these parameters were compiled from previous studies carried out by INVÍAS in the study area and the analysis considers estimated values in order to observe the effects on the geotechnical dynamics of the case study. The applied process aims to approach the behavior of the slopes of the study area when precipitation variables and seismic activity of the area are analyzed. This facilitates failure forecasting in instability zones as long as the history of mass movement records in the study area is available. For the current study, an analysis was carried out at a local scale; however, in order to involve more removal events in the study, it was proposed to frame the road corridor with a grid made up of 1km^2 cells. This generalizes the probabilistic analysis and could reduce the quality of the estimate made due to the size of the cell considered.

The emergence of mass movements triggered by the accumulated rainfall of 3 days and preceding 15 days is possible, according to the fault threshold calculated due to the observation in the behavior of the probability of saturation where the values of greater probability coincide with the critical points identified in the visual inspection carried out in the Tunja-Páez road corridor. When considering the seismic acceleration of 0.2g at all points of mass removal, it was observed that the probabilities due to seismic action in normal humidity or unsaturated conditions had a maximum value of 80% and the scenario becomes critical when the height of the assumed water table (Hw=5m), reaching a probability per action of the earthquake in saturated condition of 94%.

When the probability of total annual failure (PFTA) is recalculated by incorporating the probabilities of saturation (Ps) for each of the Climate Change scenarios, it is observed that the variation of the probability between scenarios is low since the results vary between 0.15% and 0.23% in relation to the scenario without Climate Change. The current study can be considered a preliminary stage of hazard studies due to mass movements in the department of Boyacá and can be improved if the information of all the prevailing soil tests in the region is available. However, it is close to a simulation of the effects of precipitation and earthquakes on the slopes of the analyzed area.

Acknowledgments

This study was supported by the Vicerrectoría de Investigación y Extensión (VIE) of the Universidad Pedagógica y Tecnológica de Colombia (UPTC) Tunja campus in collaboration with public entities such as the Secretaría de Infraestructura de Boyacá and the Instituto Nacional de Vías (INVIAS).

References

[1] Vano, A., Dettinger, M., Cifelli, R., Dufour, A., Miller, K., Olsen, J., and Wilson, A., Hydroclimatic extremes as challenges for the water management community: lessons from Oroville and hurricane Harvey, Explaining extreme events of 2017 from a climate perspective, Bull.

Amer. Meteor. Soc, 100(1), pp. S9-S14, 2019. DOI: https://doi.org/10.1175/BAMS-D-18-0219.1

[2] Panel Intergubernamental de Cambio Climático (IPCC). Calentamiento global de 1.5°C: informe especial sobre los efectos del calentamiento global con respecto a los niveles preindustriales y las trayectorias correspondientes que deberían seguir las emisiones mundiales de gases de efecto invernadero, en el contexto del reforzamiento de la respuesta mundial a la amenaza del cambio climático, el desarrollo sostenible y los esfuerzos por erradicar la pobreza. [en línea]. 2019. ISBN 978-92-9169-351-1. Disponible en: https://www.ipcc.ch/site/assets/uploads/sites/2/2019/09/IPCC-Special-Report-1.5-SPM_es.pdf.

[3] Greenpeace. Así nos afecta el cambio climático. Informe. [en línea]. 2018. Disponible en: https://es.greenpeace.org/es/wp-content/uploads/sites/3/2018/11/GP-cambio-climatico-LR.pdf.

[4] United Nations Office for the Coordination of Humanitarian Affairs (OCHA). Temporada de lluvias 2010 Fenómeno de La Niña. Informe de Situación No 6, pp. 2-7, [en línea]. 2010. Disponible en: https://www.paho.org/disasters/index.php?option=com_docman&view=download&category_slug=colombia&alias=1630-informe-ocha-colombia-ola-invernal&Itemid=1179&lang=en.

[5] Instituto de Hidrología Meteorología y Estudios Ambientales - IDEAM y Universidad Nacional de Colombia - UNAL. La variabilidad climática y el cambio climático en Colombia. IDEAM Bogota, [en línea]. 2018. Disponible en: https://documentacion.ideam.gov.co/cgi-bin/koha/opac-detail.pl?biblionumber=38256.

[6] Departamento Nacional de Planeación DNP. Índice municipal de riesgo de desastres de Colombia. [en línea]. 2018. Disponible en: https://colaboracion.dnp.gov.co/CDT/Prensa/Presentaci%C3%B3n%20%C3%8D%C3%8Dndice%20Municipal%20de%20Riesgo%20de%20Desastres.pdf

[7] Departamento Nacional de Planeación DNP. Índice Municipal de riesgos de desastres ajustado por capacidades. [en línea]. 2019. Disponible en: https://colaboracion.dnp.gov.co/CDT/Prensa/IndiceMunicipaldeRiesgodeDesastres.pdf

[8] Cámara de Comercio de Tunja, Cámara de Comercio de Duitama, Cámara de Comercio de Sogamoso y Fundación Centro de Desarrollo Tecnológico para la Sostenibilidad y Competitividad Regional. Boyacá en cifras. [en línea]. 2019. ISSN: 2539-150X, Disponible en: https://cctunja.org.co/wp-content/uploads/2019/09/Boyaca_Cifras_2019_.pdf

[9] Instituto Distrital de Gestión de Riesgos y Cambio Climático IDIGER. Escenario de Riesgo, Riesgo por Movimientos en Masa. [en línea]. 2020. Disponible en: https://www.idiger.gov.co/rmovmasa.

[10] Mergili, M., Marchant, C.I., y Moreiras, S.M., Causas, características e impacto de los procesos de remoción en masa, en áreas contrastantes de la región Andina. Cuadernos de Geografía. Revista Colombiana de Geografía. 24(2), pp. 113-131, 2014. DOI: https://doi.org/10.15446/rcdg.v24n2.50211.

[11] Banco Mundial Colombia y Global Facility for Disaster Reduction and Recovery (GFDRR). Análisis de la gestión del riesgo de desastres en Colombia: un aporte para la construcción de políticas públicas. 1ra ed. [en línea]. 2012. Disponible en: https://gestiondelriesgo.gov.co/sigpad/archivos/gestiondelriesgoweb.pdf

[12] Bornaetxea, T., Antigüedady, I., y Ormaetxea, O., Mapas de susceptibilidad de deslizamientos a partir del modelo de regresión logística en la cuenca del río Oria (Gipuzcoa). Estrategias de tratamiento de variables. Cuaternario y Geomorfología. 32(2), pp. 7-29, 2018. DOI: https://doi.org/10.17735/cyg.v32i1-2.59493.

[13] Tsangaratos, P., Ilia, I., Hong, H., Chen, W., and Xu, C., Applying information theory and GIS-based quantitative methods to produce landslide susceptibility maps in Nancheng Country, China. Landslides. 14, pp. 1091-1111, 2016. DOI: https://doi.org/10.1007/s10346-016-0769-4.

[14] Instituto Nacional de Vías INVÍAS y TECNOCONSULTA. Actualización de los estudios y diseños para el mejoramiento de la carretera Tunja - Ramiriquí - Miraflores -Páez entre el PR0 y el PR118. Vol. 14, Hito III, 2014, 15 P.

[15] Rojas, J., and Leguizamón, L.C., A review of the relation between climate variability and mass removal processes: Tunja-Páez case study, Ingeniería Solidaria. 18(1), pp. 1-40, 2022. DOI: https://doi.org/10.16925/2357-6014.2022.01.09.

[16] Hidalgo, C. y Vega, J., Estimación de la amenaza por deslizamientos detonados por sismos y lluvia (Valle de Aburrá, Colombia). Revista EIA. [en línea]. 11(22), pp. 103-117, 2014. Disponible en: https://revistas.eia.edu.co/index.php/reveia/article/view/676.

[17] Hidalgo, C., Vega, J., De Assis, A.P. y Villarraga, M.R., Estimación por deslizamiento en proyectos lineales: carreteras en suelos residuales. Conferencia: IV Simposio Panamericano de Deslizamientos. [en línea]. 2012, pp. 1-19, Disponible en: https://www.researchgate.net/publication/294874206.

[18] Moreno, H., Vélez, M.V., Montoya, J. y Rhenals, R.L., La lluvia y los deslizamientos de tierra en Antioquia: análisis de su ocurrencia en las escalas interanual, intra anual y diaria. Revista EIA. [en línea]. (5), pp. 59-69, 2006. Disponible en: https://www.scielo.org.co/pdf/eia/n5/n5a05.pdf.

[19] Aristizábal, E., González, T., Montoya. J., Vélez, J., y Martínez-Guerra, A., Análisis de umbrales empíricos de lluvia para el pronóstico de movimiento en masa en el Valle de Aburrá, Colombia. Revista EIA, [en línea]. (15), pp. 95-111, 2011. Disponible en: https://www.scielo.org.co/pdf/eia/n15/n15a09.pdf

[20] Ramos, A.M., Trujillo, M.G. y Prada, L.F., Niveles umbrales de lluvia que generan deslizamientos: una revisión crítica. Ciencia e Ingeniería Neogranadina. 25(2), pp. 61-80, 2015. DOI: https://doi.org/10.15665/re.v13i1.348.

[21] Althuwaynee, O.F., Asikoglu, O., and Eris, E., Threshold contour production of rainfall intensity that induces landslides in susceptible regions of northern Turkey. Landslides, [online]. 15(8), pp. 1541-1560, 2018. Available at: https://link.springer.com/article/10.1007/s10346-018-0968-2

[22] Vega, J.A., Estimación del riesgo por deslizamientos de laderas generados por eventos sísmicos en la ciudad de Medellín usando herramientas de Geomática. Tesis de Maestría, Universidad Nacional de la Plata, Argentina. [en línea]. 2013. Disponible en: https://comisiones.ipgh.org/CARTOGRAFIA/Premio/Tesis_2015/Tesis_Johnny_Vega.pdf.

[23] Servicio Geológico Colombiano (SGC). Guía metodológica para estudios de amenaza, vulnerabilidad y riesgo por movimientos en masa 1ra ed. ISBN: 978-958-99528-5-6, 2016.

[24] Asociación colombiana de Ingeniería Sísmica AIS. Estudio General de Amenaza Sísmica de Colombia 2009. Comité AIS-300: amenaza sísmica, Bogotá, Colombia. [en línea]. pp. 95-96, 2009. Disponible en: https://www.rcrisis.com/Content/files/EstudioGeneraldeAmenazaSismicadeColombia2009_AIS_lowres.pdf.

[25] Keefer, D.K., Landslides caused by earthquakes. Geological Society of America Bulletin. 95(4), pp. 406–421, 1984.

[26] Baecher, G., and Christian, J., Reliability and Statistics in Geotechnical Engineering. Wiley. ISBN: 978-0-470-87125-6, 2003.

[27] Hidalgo, C. y De Assis, A.P., Herramientas para análisis por confiabilidad en geotecnia: la teoría. Revista Ingenierías Universidad de Medellín. [en línea]. 10(18), pp. 69-78, 2011. Disponible en: https://revistas.udem.edu.co/index.php/ingenierias/article/view/339.

[28] Rosales-Rodríguez, C.A., Hazard maps of shallow landslides associated with infiltration processes in the Sapuyes river basin. Ingeniería e Investigación, 41(1), pp. 1-9, 2021. DOI: https://revistas.unal.edu.co/index.php/ingeinv/article/view/84611/77531

[29] Chowdhury, R., Flentje, P., and Bhattacharya, G., Geotechnical Slope Analysis. 1st ed. Taylor & Francis, 2006. DOI: https://doi.org/10.1201/9780203864203.

J.K. Rojas-Mesa, is BSc. Eng in Transportation and Roads Engineer, Sp. in Road Infrastructure, MSc. in Engineering with emphasis on Road Infrastructure, with experience in analysis in probabilistic estimation of mass movements triggered by precipitation and earthquakes and construction processes. Co-researcher of the Road Infrastructure Research and Development Group of the Universidad Pedagógica y Tecnológica de Colombia (UPTC).
ORCID: 0000-0003-0779-3843

L.C. Leguizamón-Barreto, is Bsc. Eng in in Transport and Roads Engineer, Sp. in Road Infrastructure, MSc., and Dr. in Engineering with emphasis in Geotechnics, with experience in modeling the mechanical behavior of geomaterials and implementation of 3D finite elements. Professor and researcher UPTC.
ORCID: 0000-0002-3316-3768

L.A. Vega-Báez, Transportation and Roads Engineer, Dr. in Engineering, UPM-Madrid – Spain, MSc. in Engineering and research in traffic and transportation, Universidad del Cauca, Sp. in Social evaluation of projects, Universidad de Los Andes. Professor and researcher UPTC.
ORCID: 0000-0001-7343-5791